Journal of High Energy Astrophysics ••• (••••) •••–•••

Contents lists available at ScienceDirect

Journal of High Energy Astrophysics

www.elsevier.com/locate/jheap

Review

Are short Gamma Ray Bursts similar to long ones?

G. Ghirlanda *, M.G. Bernardini, G. Calderone, P. D'Avanzo

INAF–Osservatorio Astronomico di Brera, Via E. Bianchi 46, I-23807 Merate (LC), Italy

ARTICLE INFO

Article history:
Received 5 March 2015
Accepted 8 April 2015
Available online xxxx

ABSTRACT

The apparent separation of short and long Gamma-Ray Bursts (GRBs) in the hardness ratio vs duration plot has been considered as a direct evidence of the difference between these two populations. The origin of this diversity, however, has been only confirmed with larger GRB samples but not fully understood. In particular, the hardness ratio is only a proxy of the shape of the spectra of GRBs and itself, together with the observed duration, does not consider the possible different redshift distribution of short and long bursts, which might arise from their different progenitors' nature. By correcting the spectral shape of short and long GRBs for the redshift effects, short GRBs are harder than long ones due to a harder low energy spectral component while the two populations have similar (rest frame) peak energy. In the rest frame, the temporal break of the long/short duration distribution is blurred away and short and long GRBs have a continuous differential duration distribution. Moreover, they show similar luminosities but their energetics differ by a factor proportional to their different average duration. The spectral evolution of long GRBs shows that the initial phase (of the order of 0.3 s rest frame) has similar spectral properties of that of short GRBs. As a consequence, the different hardness at low energies might be due to a prolonged spectral evolution of long GRBs with respect to short ones. Finally, we show that long GRBs can have a null lag similarly to short bursts. Moreover, we find that a considerable fraction of long (and most of short) GRBs are inconsistent with the lag-luminosity relation which could be a boundary in the corresponding plane, rather than a correlation.

1. Introduction

Gamma Ray Bursts (GRBs) are typically divided into two classes of short and long events based on their observed duration in the γ-ray band. The bimodal distribution of T_{90}, i.e. the timescale in which from 5% to 95% of the counts are recorded, suggested a possible separation at $\sim$2 s (Kouveliotou et al., 1993). For a recent review of Short GRBs see Berger (2014). This was assumed for years as the dividing line between short (SGRB with $T_{90} \leq 2$ s) and long (LGRB with $T_{90} > 2$ s) GRBs. A statistically significant (10^{-4}) intermediate duration population was also claimed (Horváth, 1998; Řípa et al., 2009) although it showed similar properties to the class of long GRBs (de Ugarte Postigo et al., 2011).[1] The apparent separation between SGRBs and LGRBs, discovered in the GRB population detected by BATSE/CGRO, was confirmed by Hete-2 (Sakamoto et al., 2005; Pélangeon et al., 2008), BeppoSAX (Frontera et al., 2009), Integral (Bošnjak et al., 2014; Savchenko et al., 2012), Swift (Sakamoto et al., 2005) and Fermi (von Kienlin et al., 2014). However, the comparison of the duration distributions of bursts detected by different instruments suffers from instrumental biases induced by the energy range where they operate, the trigger method (image triggers are less sensitive to short/spiky bursts) and the energy range where the T_{90} is computed (on average a smaller T_{90} is estimated with light curves of higher energy photons – Qin et al., 2013).

What, observationally, does distinguish short and long bursts in addition to their duration? It was early realised that SGRBs might have different spectral properties. The hardness ratio (HR), defined as the ratio of the flux in two separated energy bands (i.e. the counts in the harder energy band divided by those in the softer), showed that short GRBs have *on average* a larger HR than long bursts (Kouveliotou et al., 1993; Tavani, 1998). However, no correlation between HR and duration was found within the individual classes (Qin et al., 2001). Fig. 1 (Sakamoto et al., 2005) shows the HR-T_{90} plot of GRBs detected by Swift (five year catalog of 476 events – grey symbols), compared with BATSE (red symbols), Beppo/SAX (green symbols) and Hete-2 (blue symbols) bursts. For Swift bursts, the Kolmogorov–Smirnov (KS) test of the HR between SGRBs and LGRBs has a probability of 8.3×10^{-20} that

* Corresponding author.
E-mail address: giancarlo.ghirlanda@brera.inaf.it (G. Ghirlanda).

[1] Recently, it has also been claimed the existence of a distinct population of ultra-long GRBs (Levan et al., 2014).

http://dx.doi.org/10.1016/j.jheap.2015.04.002
2214-4048/

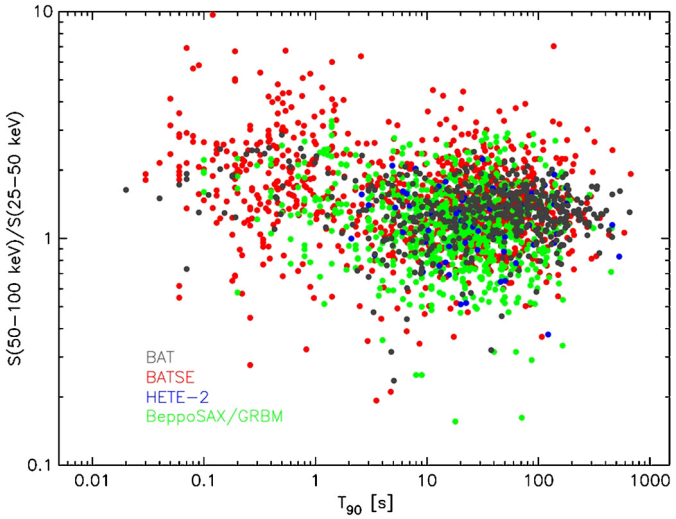

Fig. 1. HR-T_{90} plot of GRBs detected by different missions (as shown in the legend) from Sakamoto et al. (2011). (For interpretation of the references to color in this figure, the reader is referred to the web version of this article.)

the two populations are drawn from the same parent distribution. In general, the populations of GRBs detected by different instruments overlay in the HR-T_{90} plane although the relative number of short and long GRBs differ among different instruments. The four year catalog of 954 Fermi bursts (von Kienlin et al., 2014) contains between 13% and 20% of SGRB with average duration ∼0.7 s and average HR>1 (LGRBs have an average duration of 25 s and HR<1).[2]

Other possible differences in the temporal properties are the smaller minimum variability timescale (MacLachlan et al., 2012, 2013) of SGRBs (on average 10 ms) with respect to LGRBs (200 ms); see also Nakar and Piran (2002) and Golkhou and Butler (2014). What links temporal and spectral properties is the lag: this is the delay (either positive or negative) between the light curves in two different energy bands. It was early found in the BATSE GRB sample that LGRBs have positive lags with the high energy light curve lagging the low energy one, while typically SGRBs have null lag (Cheng et al., 1995; Norris et al., 2001; Norris and Bonnell, 2006).

Overall, the comparison of the prompt γ-ray emission properties of short and long GRBs shows that short GRBs have (a) harder spectra (as shown by the HR, Fig. 1), (b) smaller variability timescale and (c) null lag. However, there are some caveats: T_{90} and HR are computed in the *observer frame* through the light curves accumulated by a given detector. Most often, HR has been computed as the ratio of the instrumental counts recorded in two different energy bands. With the launch of Swift in 2004 (Gehrels et al., 2004) the possible different redshift distribution of short and long bursts was disclosed. BATSE and Fermi data allowed us to characterise the spectra of GRBs over a wide (few keV to several MeV) energy range with tens of ms time resolution. We now know that GRB spectra might have different shapes (typically represented by curved models, i.e. more complicated than simple powerlaw) and strongly evolve with time within individual GRBs. Therefore, (1) the redshift, (2) the overall shape of the spectrum and (3) its evolution within the burst should all be considered when comparing the temporal and spectral properties of SGRB and LGRB. The possible different redshift distributions of short and long GRBs might change the results, i.e. blur away or exacerbate the differences between the two classes. The HR represents only a proxy of the real spectral diversity of short and long events which should instead be searched in the difference of the spectral parameters of these classes (Ghirlanda et al., 2004, 2009, 2011).

In the following sections we will progressively probe deeper into the consolidated differences of short and long GRBs exploring the origin of the different HR by searching for differences in the spectral shape (Section 2), including the redshift corrections (Section 3) and the temporal evolution of the spectrum (Section 4) and, finally, revisiting the lag as a discriminator between short and long events (Section 5).

2. The observed spectrum of GRBs

Spectral analysis of samples of short and long GRBs showed that this is typically represented by a curved function (Preece et al., 2000; Ghirlanda et al., 2002, 2004; Kaneko et al., 2006; Frontera et al., 2009; Nava et al., 2011a; Goldstein et al., 2013, 2012; Gruber et al., 2014). In particular, a smoothly broken power law (Band et al., 1993) or a power law with a high energy cut-off suffice to reproduce the observed spectra of most short and long GRBs with the former being more often fitted by a cutoff power law function (Ghirlanda et al., 2004, 2009). The common feature of these functions is the presence of a low energy power law (parametrised by its photon spectral index α) and a characteristic energy $E_{\rm peak}$ where the νF_ν spectrum peaks. The smoothly broken power law model has an additional high energy power law component (parametrised by the photon spectral index β).

Spectral analysis of samples of short and long GRBs detected by BATSE and Fermi (Ghirlanda et al., 2004, 2009) shows that short and long GRBs have slightly different $E_{\rm peak}$ distributions (with a KS probability of 10^{-2} of being drawn from the same parent population) while the main difference is in the low energy spectral index (α) distribution (with a KS probability of 10^{-4}). From the distributions of these two spectral parameters (Ghirlanda et al., 2009) it *appears* that SGRBs are harder than LGRBs due both to a combination of their peak energy (on average $E_{\rm peak}\sim 400$ keV for SGRBs with respect to 220 keV for long events) and of a harder low energy spectral index (on average $\alpha\sim -0.4$ for SGRBs with respect to -0.92 for long ones). These results, found in the BATSE short and long populations (Ghirlanda et al., 2009), are confirmed by the Fermi data (Nava et al., 2011a). Fig. 2 shows the distributions of the low energy spectral index (top panel) and peak energy (bottom panel) of Fermi long (blue hatched histogram) and short (red hatched histogram) bursts (from Nava et al., 2011a).[3] The top panel of Fig. 2 also shows that all short GRBs have a low energy spectral index violating (i.e. harder than) the synchrotron limit of -1.5 in case of electron cooling.

We further test these results with the most updated sample of GRBs from the GBM/Fermi catalog[4] (von Kienlin et al., 2014; Gruber et al., 2014). We selected all the GRBs (up to Feb. 2015) detected by the GBM on board Fermi with a time integrated spectrum well fitted by either a Band function or a power law with exponential cutoff. Fig. 3 (top panel) shows the low energy spectral index (α) versus the peak energy ($E_{\rm peak}$) *in the observer frame* for the 982 GRBs. Red and blue symbols show the population of short and long events, respectively, considered separating the sample at 2 s. The KS test probabilities of $E_{\rm peak}$ and α for the two populations are 10^{-30} and 10^{-24}, respectively. We also verified if the KS probability depends on the 2 s short/long divide. Indeed, it has been suggested (Bromberg et al., 2012, 2013) that there could be a contamination of collapsars (i.e. long GRB progenitors) in the

[2] The HR values may change according to the energy ranges selected for their computation.

[3] For a comparison of the spectral properties of short and long GRBs detected by Fermi and BATSE see Nava et al. (2011b).

[4] http://heasarc.gsfc.nasa.gov/W3Browse/fermi/fermigbrst.html.

Please cite this article in press as: G. Ghirlanda et al., Are short Gamma Ray Bursts similar to long ones?, J. High Energ. Phys. (2015), http://dx.doi.org/10.1016/j.jheap.2015.04.002

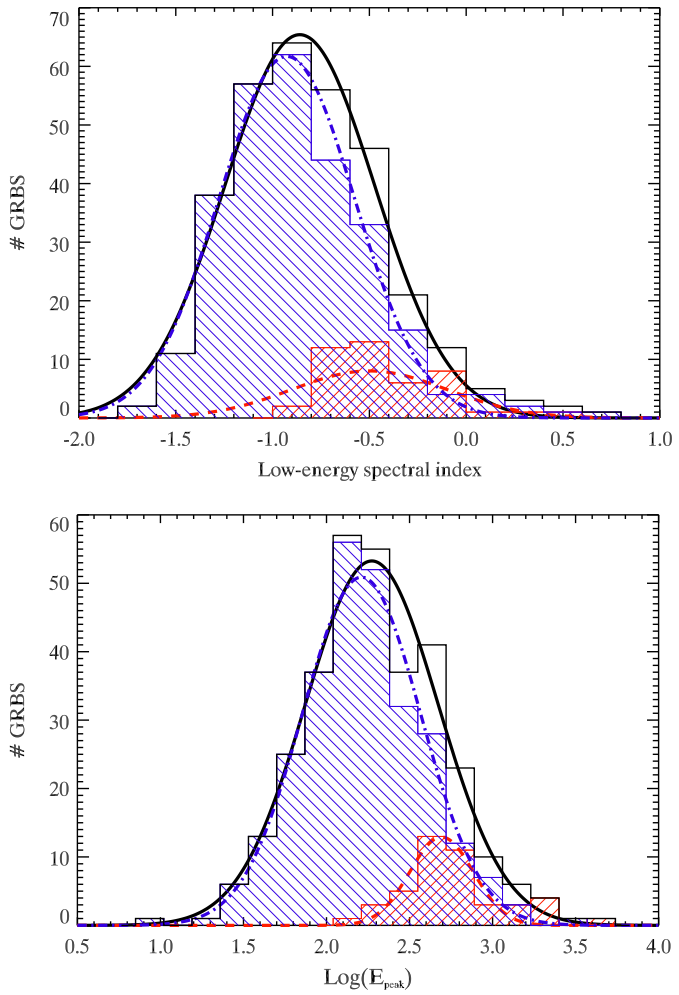

Fig. 2. Time integrated spectral parameters of short GRBs (red hatched histograms) versus long GRBs (blue hatched histograms) detected by Fermi and analysed by Nava et al. (2011a, 2011b). The top and bottom panels shows the low energy spectral index and the peak energy of the νF_ν spectrum, respectively. (For interpretation of the references to color in this figure legend, the reader is referred to the web version of this article.)

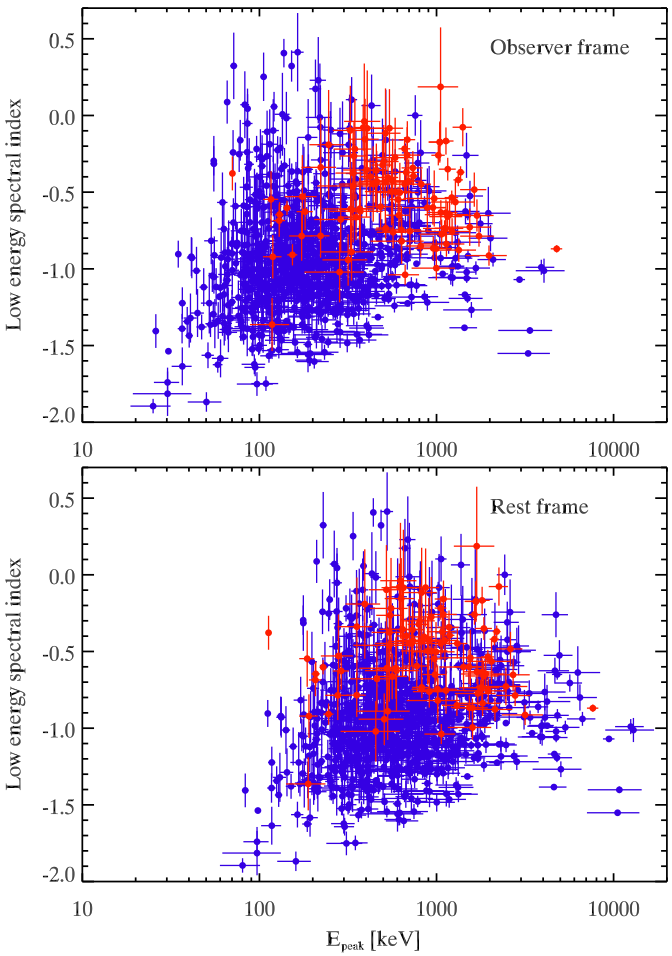

Fig. 3. Low energy spectral index versus peak energy in the observer frame (top panel) and in the rest frame (bottom panel) for the present sample of Fermi GRBs with time integrated spectrum fitted with either a Band model or a cutoff power law model. Red and blue symbols are for short and long GRBs, respectively. (For interpretation of the references to color in this figure legend, the reader is referred to the web version of this article.)

population of short events and that the separation between the two classes might differ by 2 s (e.g. 0.8 for Swift). We find that by shifting the long/short divide by a factor of 2 the KS probability remains highly significative of the diversity of the spectral parameters of the two classes.

3. Rest frame properties of short GRBs

The comparison of the observed properties (e.g. T_{90} and spectral parameters) of short and long GRBs does not take into account the redshift effects. In particular the observed duration and the observed peak energy depend on the source redshift. If short and long GRBs have different redshift distributions, this effect can considerably blur away the differences discussed in the previous section.

However, our knowledge of the distribution of GRBs through cosmic times is still limited by the fact that the majority of the GRBs observed by *Swift* are lacking a redshift measurement (indeed the measure of the distance has been secured for about 1/3 of long GRBs and 1/4 of short GRBs). This fact strongly limits the possibility of well grounded studies aimed at shaping the GRB rest-frame properties and redshift distribution.

3.1. Spectral parameters

As a first exercise we used the average redshift of SGRB, $z = 0.6$, and LGRBs, $z = 2.1$, in order to correct the observed spectral shape of the two populations. The bottom panel of Fig. 3 shows the rest frame $E_{\rm peak}$ (i.e. corrected for the $1 + z$ factor for long and short events). Note that the slope of the spectrum below the peak (i.e. the spectral index α) is unaffected by this correction. In the rest frame, the KS probability between short and long events (keeping their separation still fixed at 2 s observed frame – i.e. considering the red and blue symbols in Fig. 3 bottom panel) reduces to 10^{-4} (to be compared to 10^{-30} in the observer frame). The KS probability on the distribution of α is instead unchanged. This result confirms that SGRBs and LGRBs have different spectra due to a different low energy spectral index rather than a different peak energy. Indeed, in the rest frame short and long GRBs (independently on their separation timescale, when it is within a factor 2 from the usual, observer frame, one – $T_{90} = 2$ s) have similar $E_{\rm peak}$ but remarkably different α with the former being harder than the latter.

3.2. Duration

The separation at 2 s between short and long GRBs was originally based on the two overlapping distributions of T_{90}. Very likely

Please cite this article in press as: G. Ghirlanda et al., Are short Gamma Ray Bursts similar to long ones?, J. High Energ. Phys. (2015), http://dx.doi.org/10.1016/j.jheap.2015.04.002

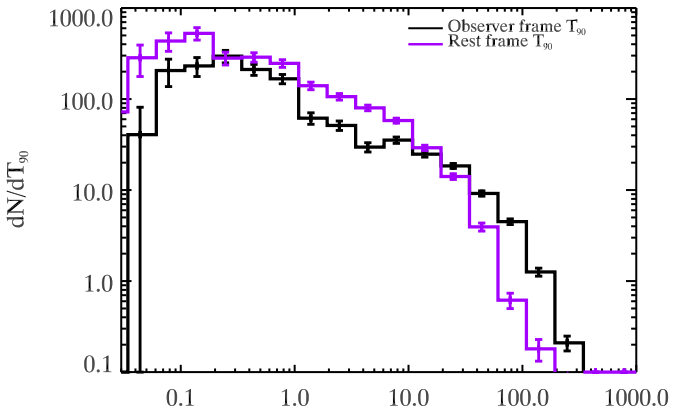

Fig. 4. Differential duration distribution of T_{90} for the GRBs in the present Fermi sample. Observed distribution (solid black line) and rest frame distribution (obtained correcting short and long GRBs for an average redshift) are shown. Vertical bars are count uncertainty in each bin. (For interpretation of the references to color in this figure, the reader is referred to the web version of this article.)

there should be a reciprocal contamination of the two populations. Bromberg et al. (2012, 2013) found that the differential distribution of the (linear rather than logarithmic) T_{90} (in the observer frame) shows a characteristic double peaked shape with a flat intermediate portion. This result was confirmed by the analysis of the T_{90} distributions of GRBs observed by BATSE, Fermi and Swift (Bromberg et al., 2013).

Fig. 4 shows the T_{90} distribution of Fermi GRBs updated to Feb. 2015: the black line represents the distribution of the observer frame T_{90}. The two populations of short and long events are clearly shown by the separation in the double peaked shape of the distribution. Indeed, long GRBs show a flat part of their duration distribution extending into that of short events. This was interpreted (Bromberg et al., 2012) as the evidence of the contamination of long GRB progenitors into the population of short GRBs. Based on these results it was proposed to better define a separation timescale (e.g. 0.8 for Swift bursts) which could minimise the fraction of collapsars in selecting samples of short events. The flat portion of the long GRB distribution was attributed to the existence of a typical timescale necessary for the jet to drill the progenitor star (for long GRBs). The break time at 10 s of the long GRB distribution between the flat and the steep portion is indeed the characteristic timescale for the jet to drill the progenitor star. If the jet lasts much longer than this timescale it will appear as a normal long GRB, if its duration is only slightly longer than this timescale it will appear a short GRB, but still produced by a collapsar.

The above considerations do not fully consider the redshift effect on the T_{90} distribution. Accounting for the possible different average redshift of the short and long GRB population, we find that the rest frame differential distribution of T_{90} is the pink solid line in Fig. 4 where the short and long GRBs do not seem to be separated any more. The flat part of the long GRB distribution completely vanishes when the rest frame duration is considered.

4. Energetics and luminosities

Short and long GRBs can also be compared in terms of energetics and luminosities. In particular this can be done in the $E_{\rm peak}$–$E_{\rm iso}$ and $E_{\rm peak}$–$L_{\rm iso}$ planes where long GRBs define two strong correlations (Amati et al., 2002; Yonetoku et al., 2004). Adding short GRBs on these planes requires the knowledge of their redshift and also a broad band spectrum which allows one to measure the peak energy and the isotropic equivalent energy $E_{\rm iso}$ and luminosity $L_{\rm iso}$. Short and long GRBs follow the same $E_{\rm peak}$–$L_{\rm iso}$ correlation but short GRBs have, on average, an energy which is smaller than that of long events by a factor comparable to the ratio of the average duration of the two populations (Ghirlanda et al., 2009). This would suggest that they might follow a correlation in the $E_{\rm peak}$–$E_{\rm iso}$ plane which is parallel to that defined by long bursts. However, these results are still limited by the small number of short GRBs with measured z and, for both classes, incomplete/inhomogeneous samples have been typically adopted.

With the aim of overcoming this problem, we selected a subsample of the full *Swift* GRB database. We considered GRBs having favourable observing conditions for ground-based redshift determination and that are bright in the 15–150 keV *Swift*/BAT band. With such criteria, we obtained two samples, consisting of 58 long GRBs[5] and 16 short GRBs, with a completeness level in redshift of 90% and 69%, respectively. The details of the two samples selection are discussed in Salvaterra et al. (2012) and D'Avanzo et al. (2014).

We used these complete samples to study the correlations between the spectral peak energy $E_{\rm peak}$ of the prompt emission, the isotropic energy $E_{\rm iso}$ and the isotropic luminosity $L_{\rm iso}$. Being free of selection effects (except for the flux limit in the 15–150 keV band), these samples provide a useful benchmark to study the rest-frame physical properties of GRBs. This enables us to probe, in an unbiased way, the issue related to the physical origin of these correlations against selection effects and firmly compares the rest frame luminosities and energetics of short and long GRBs.

We checked the consistency with the $E_{\rm peak}$–$L_{\rm iso}$ (Yonetoku et al., 2004), and with the $E_{\rm peak}$–$E_{\rm iso}$ relations (Amati et al., 2002) for all the *Swift* long GRBs with redshift[6] and the short GRBs of our sample. The results are shown in Fig. 5. All events are found to be consistent with the $E_{\rm peak}$–$L_{\rm iso}$ correlation, which is known to be valid for long GRBs (Yonetoku et al., 2004; Nava et al., 2012). By fitting together the long GRBs with redshift and the short GRBs of our sample with the function $y = 10^A x^B$ we obtain a normalisation $A = -22.98 \pm 1.81$ and a slope $B = 0.49 \pm 0.03$. A significant exception is the short GRB 080905A which lies at more than 3σ from the best fit. We note that this event has the lowest values for $E_{\rm iso}$ and $L_{\rm iso}$ among the short GRBs of our sample. We speculate that the redshift of this GRB might be higher than the value inferred from its (possibly chance) association with a nearby ($z = 0.122$) spiral galaxy observed edge-on (D'Avanzo et al., 2014). We also found evidence for a $E_{\rm peak}$–$L_{\rm iso}$ correlation followed by short GRBs being systematically fainter than the correlation defined by long GRBs. Although such finding is intriguing, we caution that it can be affected by the choice of the temporal bin in the estimate of the isotropic peak luminosity for both long and short GRBs (by choosing smaller and smaller bins, the estimate of $L_{\rm iso}$ tends to increase). In Fig. 5 (right panel) we divided the short GRBs with $\Delta t \geq 1000$ ms (red circle), $50 \leq \Delta t \leq 64$ ms (green diamonds), $\Delta t = 16$ ms (yellow triangles) and $\Delta t = 4$ ms (purple upside down triangle). For the majority of long bursts the peak flux has been estimated on a $\Delta t \sim 1$ s timescale. We find that short GRBs with smaller Δt systematically tend to have larger $L_{\rm iso}$, and to be more consistent with the best fit of long bursts. These preliminary results suggest that a consistency between the long and short $E_{\rm peak}$–$L_{\rm iso}$ correlation can be reached by considering for both classes of events a Δt which is a (proper) fraction of their T_{90} (Tsutsui et al., 2013; D'Avanzo et al., 2014).

Concerning the $E_{\rm peak}$–$E_{\rm iso}$ plane, short GRBs define a region with the same slope measured for the correlation holding for long GRBs but with a different normalisation, lying systematically on

[5] Up tp March 2012; since then the sample increased, consisting now of 100 bursts, 82% with redshift.

[6] As reported in Nava et al. (2012), the $E_{\rm peak}$–$L_{\rm iso}$ was found to hold for both the total sample of *Swift* long GRBs with redshift and for our complete (flux-limited) sample, with the same values of slope and normalisation.

Please cite this article in press as: G. Ghirlanda et al., Are short Gamma Ray Bursts similar to long ones?, J. High Energ. Phys. (2015), http://dx.doi.org/10.1016/j.jheap.2015.04.002

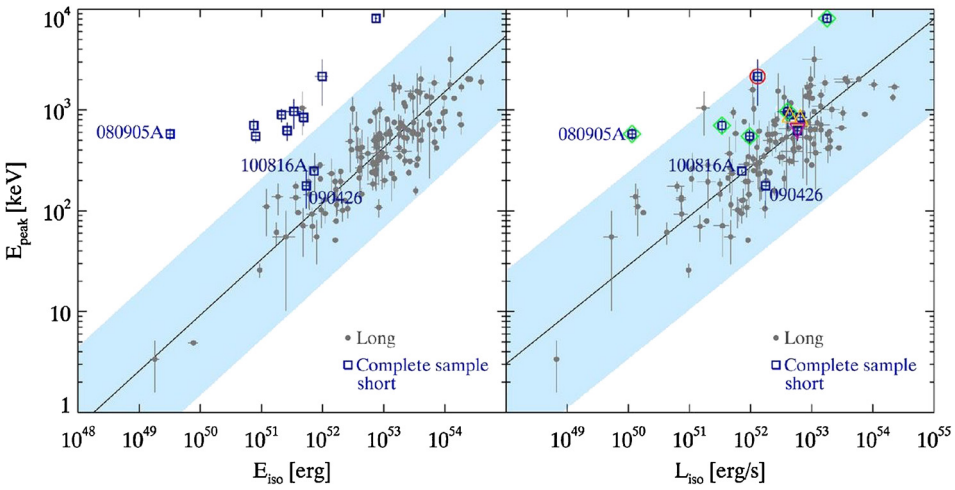

Fig. 5. $E_{\rm peak}$–$E_{\rm iso}$ (*left panel*) and $E_{\rm peak}$–$L_{\rm iso}$ (*right panel*) correlations (dots: long GRBs, data taken from Nava et al., 2012; empty squares: short GRBs, data taken from (D'Avanzo et al., 2014). The power-law best fit is shown as a solid dark line. The shaded region represents the 3σ scatter of the distribution. Two GRBs with uncertain classification (GRB 090426 and GRB 100816A) and a possible outlier of the $E_{\rm peak}$–$L_{\rm iso}$ correlation (GRB 080905A) are also marked. (For interpretation of the references to color in this figure, the reader is referred to the web version of this article.)

the left with respect to the best fit line of long GRBs. Two exceptions are GRB 090426 and GRB 100816A, both consistent within 2σ confidence region of the relation holding for long GRBs. As discussed in D'Avanzo et al. (2014), both these events have an uncertain classification. In light of its duration (T_{90} of 2.9)[7] and prompt emission properties, GRB 100816A is likely a long-duration event. No firm conclusion can be derived for the classification of GRB 090426, mainly due to the lack of strong constraints on the properties of its prompt emission spectrum. A fit to the short GRBs of the *complete* sample in the $E_{\rm peak}$–$E_{\rm iso}$ plane with the function $y = 10^A x^B$ provides a normalisation $A = -28.01 \pm 2.91$ and a slope $B = 0.60 \pm 0.06$. As a comparison, as reported in Nava et al. (2012), the same fit performed on the complete sample of LGRBs provides $A = -29.60 \pm 2.23$ and $B = 0.61 \pm 0.04$.

5. Long "start" as short

As discussed in Section 3, short GRBs spectra show harder low-energy spectral index, and a slightly higher peak energy, when compared to the time integrated spectra of long GRBs. However, considering only the spectra corresponding to the first 1–2 s (in the observer frame) of long GRBs, the distributions of both the low-energy spectral index and the peak energy become indistinguishable from those of short GRBs (Ghirlanda et al., 2004, 2009). The total energy emitted by short GRBs (for which we have a redshift estimate) is significantly lower than for a typical long GRB, however the involved luminosities are comparable, and both short and long GRBs appear to follow the same $E_{\rm peak}$–$L_{\rm iso}$ relation (Section 4, Fig. 5). Moreover, by performing a time resolved spectroscopy of short GRBs it has been shown that the peak energy tracks the flux evolution and, in the few cases where a redshift is available, the $E_{\rm peak}(t)$–$L_{\rm iso}(t)$ correlation for short GRBs is similar to the one for long GRBs (Ghirlanda et al., 2011). Finally, both short and long GRBs lie on the three parameter correlation $E_{\rm X,iso}$–$E_{\gamma,\rm iso}$–$E_{\rm peak}$ (Bernardini et al., 2012; Margutti et al., 2013). These results suggest that the emission mechanism in both short and long GRBs might be similar, although occurring on different timescales, the latter being likely related to the different lifetime of their progenitor engines (Ghirlanda et al., 2009, 2011; Guiriec et al., 2010, 2013).

In Calderone et al. (2015) we further explore these similarities by comparing the intrinsic (i.e. rest frame) spectral properties $E_{\rm peak}$, $L_{\rm iso}$ and $E_{\rm iso}$ of the short GRBs with those of *the beginning of long GRBs*, evaluated by integrating the spectra on a rest frame time scale equal to the typical duration of short events. Although there is not a universal short burst duration, a reasonable choice is to use the average rest frame duration ($T_{90}/(1+z)$) of short GRBs. For the sample of short GRBs with redshift in D'Avanzo et al. (2014) This duration is 0.3 s.

For the comparison we considered two samples of short and long GRBs respectively:

- the short GRB sample comprises 9 bursts from the D'Avanzo et al. (2014) sample and 3 more bursts detected by *Fermi*/GBM. We considered the spectral properties reported in D'Avanzo et al. (2014) for the 9 burst in that paper, and we analysed the *Fermi*/GBM data for the remaining bursts. These results are collectively referred to as the *short* results;
- the long GRB sample comprises 44 bursts detected by *Fermi*/GBM up to December 2013. For these bursts we performed two spectral analyses on the *Fermi*/GBM data: one on the time integrated spectra (*whole* results) and one by considering just the data collected during the first 0.3 s rest frame (corresponding to $0.3 \times (1+z)$ s in the observer frame) of the burst (*first* results).

For the spectral analysis, we considered the time selection given in Gruber et al. (2014) for the bursts common to both our sample and their catalog. For the other GRBs we performed a visual inspection of the light curves to identify the time interval where the counts are significantly above the background. For the *first* analysis we considered the first occurrence of a 0.3 s long (rest frame) time bin whose total counts are significantly above the background (at 3σ level).

The spectral models used for fitting are custom[8] versions of either the cutoff power law or the Band model, in which we adopt the logarithm of the peak energy (`log_Ep`) and of the integrated flux (`log_F`) in the rest frame energy range 1 keV–10 MeV, as free parameters in the fit. The best fit value of `log_F` allows to estimate the intrinsic isotropic luminosity $L_{\rm iso} = 4\pi D_{\rm L}^2 \times F$ and

[7] In spite of a duration larger than 2 s, GRB 100816A was initially classified as a short GRB (Norris et al., 2010).

[8] The implementation of these spectral models suitable to be used in XSPEC is available at http://www.giorgiocalderone.url.ph/xspec_ggrb.tar.gz.

Please cite this article in press as: G. Ghirlanda et al., Are short Gamma Ray Bursts similar to long ones?, J. High Energ. Phys. (2015), http://dx.doi.org/10.1016/j.jheap.2015.04.002

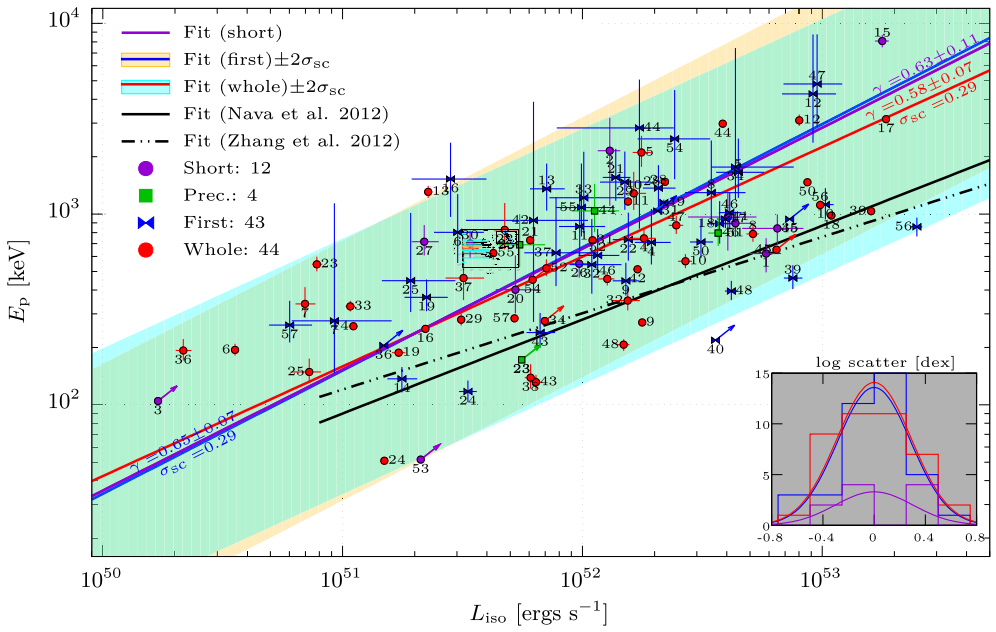

Fig. 6. Results of the spectral analysis in the $E_{\rm peak}$–$L_{\rm iso}$ plane. The *short*, *first* and *whole* results are shown with purple, blue and red symbols respectively. The best-fit $E_{\rm peak}$–$L_{\rm iso}$ correlations are shown as solid lines with the corresponding colours and the inset plot shows the histograms of residuals. The slope (γ) and scatter ($\sigma_{\rm sc}$) of the correlations are shown at the edges of the figure. The $2\sigma_{\rm sc}$ scatter of the *first* and *whole* results are shown as orange and cyan shaded area respectively. The $E_{\rm peak}$–$L_{\rm p,iso}$ relations from the total sample of Nava et al. (2012) (black dashed line) and from the combined short and long GRB sample of Zhang et al. (2012) (double dot–dashed lines) are also shown for comparison. Lower limits and precursors are shown with arrows and green symbols respectively. (For interpretation of the references to color in this figure legend, the reader is referred to the web version of this article.)

its uncertainty, without propagating the uncertainties on the other parameters. We used `xspec`, ver. 12.8.1g to minimise the C-STAT value when comparing the sum of folded spectral model and background expected counts with the observed data.

Fig. 6 shows the results of the spectral analysis in the $E_{\rm peak}$–$L_{\rm iso}$ plane. The *short*, *first* and *whole* results are shown with purple, blue and red symbols respectively. The best-fit $E_{\rm peak}$–$L_{\rm iso}$ correlations are shown as solid lines with the corresponding colours and the inset plot shows the histograms of residuals. The slope (γ) and scatter ($\sigma_{\rm sc}$) of the correlations are shown at the edges of the figure. The $2\sigma_{\rm sc}$ scatter of the *first* and *whole* results are shown as orange and cyan shaded area respectively. The $E_{\rm peak}$–$L_{\rm p,iso}$ relations from the total sample of Nava et al. (2012) (black dashed line) and from the combined short and long GRB sample of Zhang et al. (2012) (double dot-dashed lines) are also shown for comparison. Lower limits and precursors are shown with arrows and green symbols respectively.

The $E_{\rm peak}$ and $L_{\rm iso}$ quantities for both the *whole* and *first* results show a robust correlation with a chance probability of being spurious of 4×10^{-7} and 10^{-3} respectively. While the former is reminiscent of the Yonetoku relation (Section 3, Yonetoku et al., 2004), the latter is a newly identified $E_{\rm peak}$–$L_{\rm iso}$ relation holding during the first 0.3 s (rest frame) of all considered bursts. Our *short* GRB sample is too small to provide a strong evidence for the existence of a similar correlation ($P_{\rm chance}=0.14$). Nevertheless all short GRBs lie within the same region identified by the $2\sigma_{\rm sc}$ region of the correlations for the long GBRs, and seem to follow the same trend.

Similar considerations apply when considering the $E_{\rm peak}$–$E_{\rm iso}$ relations: both the *first* and *whole* results show strong correlations, while the *short* is only marginally significant. However, in the $E_{\rm peak}$–$E_{\rm iso}$ plane the *first* and *short* bursts lie on the same region, and are significantly away from the *whole* relation (see Calderone et al., 2015 for details).

In summary, when considering the intrinsic $E_{\rm peak}$, $E_{\rm iso}$ and $L_{\rm iso}$ spectral quantities, the spectra of both the short GRBs and the first 0.3 s (rest frame) of long ones are actually indistinguishable, despite the likely different progenitors and different total energy involved. In particular, if a long GRB (whatever its progenitor) should last less than $\sim$ 0.3 s (rest frame) we would not be able to distinguish it from a short GRB with current detectors. We note that also X-ray flares, that are though to be linked to the prompt emission, show a hard-to-soft evolution in time, albeit spanning a different energy range (e.g. Margutti et al., 2010). We identified two new $E_{\rm peak}$–$E_{\rm iso}$ and $E_{\rm peak}$–$L_{\rm iso}$ correlations valid during the first 0.3 s of long GRBs, and all the short GRBs in our sample are consistent with these relations within the scatter. These correlations suggest that a common process may be at work in both short and long GRBs.

6. Lags of short and long GRBs

The presence of a positive *spectral lag* (i.e. the delay in the arrival times of low-energy photons with respect to high-energy photons) has been considered a common feature of long GRB prompt emission (Cheng et al., 1995), and it has been used as a possible tool to discriminate between long and short GRBs (Gehrels et al., 2006), since the latter tend to have a smaller lag (consistent with zero) with respect to long GRBs (Norris et al., 2001; Norris and Bonnell, 2006).

Norris et al. (2000) showed that the positive spectral lag for long GRBs anti-correlates with the burst bolometric peak luminosity, and this anti-correlation has been explored and confirmed with different samples (see also Norris, 2002; Schaefer, 2007; Hakkila et al., 2008; Arimoto et al., 2010; Ukwatta et al., 2010). The large increase in the redshift measurements available thanks to the advent of *Swift* (Gehrels et al., 2004) allowed Ukwatta et al. (2012) to perform the first detailed analysis of the spectral lag for long GRBs, adopting two selected rest frame energy bands for all the considered burst. They confirmed the existence of the correlation with a smaller scatter when compared to previous analyses in the observer-frame (e.g. Ukwatta et al., 2010). However, in the determination of the lag-luminosity correlation they did not con-

Please cite this article in press as: G. Ghirlanda et al., Are short Gamma Ray Bursts similar to long ones?, J. High Energ. Phys. (2015), http://dx.doi.org/10.1016/j.jheap.2015.04.002

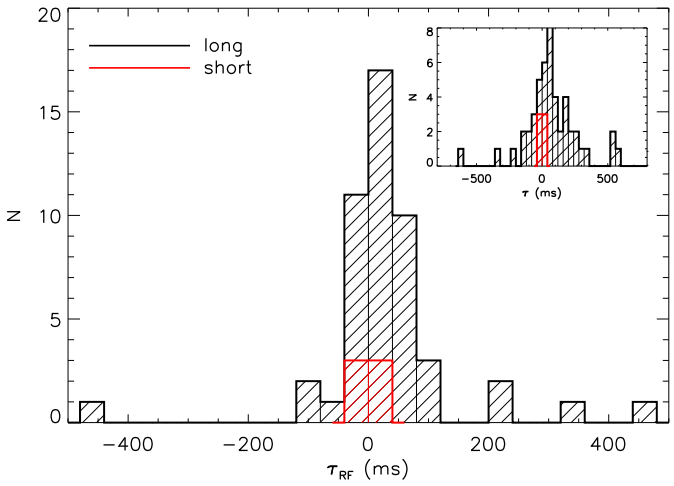

Fig. 7. Distribution of the rest-frame spectral lags. Black: 50 long GRBs from the BAT6 sample. Red: 6 short GRBs from the S-BAT4 sample. Inset: distribution of the observer-frame spectral lags. (For interpretation of the references to color in this figure legend, the reader is referred to the web version of this article.)

sider 44% of the GRBs of their original sample that have spectral lag consistent with zero or negative.

In Bernardini et al. (2015) we analysed the spectral lag for both long and short GRBs in order to investigate the opportunity to use it as a distinctive feature for these two classes of GRBs, and the role of negligible lags in the lag-luminosity plane. We considered two samples of 50 long and 6 short GRBs from the BAT6 (Salvaterra et al., 2012) and S-BAT4 (D'Avanzo et al., 2014) complete samples, respectively. Since the spectral lag value is dependent upon the energy bands chosen to compute it for both short (Abdo et al., 2009; Guiriec et al., 2010, 2013) and long GRBs (Ukwatta et al., 2010), we adopted two fixed rest-frame energy bands (100–150 keV and 200–250 keV) to perform a direct comparison of the lags of the two classes of long and short GRBs.

With the background subtracted light curves observed by the *Swift*/Burst Alert Telescope (BAT, Barthelmy et al., 2005) we computed the discrete cross-correlation function (CCF) as derived by Band (1997) to measure the temporal correlation of the two light curves in the two different energy bands. The CCF is modelled with an asymmetric Gaussian model to search for its global maximum that, by definition, corresponds to the spectral lag τ. We choose an asymmetric Gaussian model since it reflects the natural asymmetry of the CCF inherited by the asymmetry of the GRB pulses (Band, 1997). We accounted for the errors on the data points through a Monte Carlo method to estimate the uncertainty on τ (Bernardini et al., 2015).

We found that the spectral lag between the chosen rest frame energy bands for long GRBs is significantly (within 1σ) greater than zero in most cases (50%). However an equally large fraction (50%) of them is consistent with zero or negative within errors. Short GRBs have in all cases limited or no lag in the same rest frame energy bands (see Bernardini et al., 2015, therein Table 1).

The distribution of the spectral lags for short GRBs is peaked at a smaller value than the long GRB distribution (mean value of the distribution $\langle\tau^S_{RF}\rangle = (-0.61 \pm 3.87)$ ms compared to $\langle\tau^L_{RF}\rangle = (43.0 \pm 17.8)$ ms, see Fig. 7). However, there is no stronger than 2σ statistical indication that the spectral lags of short and long GRBs are drawn from two different populations: if we perform a Kolmogorov–Smirnov (KS) test, the probability that the two samples are drawn from the same population is 4.1%. The time-integrated spectral lag as a tool to distinguish between short and long GRBs might not be as definite as thought before: the existence of a large fraction of long GRBs with a lag consistent with zero makes it challenging to classify the ambiguous GRBs.

If we compare the distributions of the spectral lag in the observer frame for long and short GRBs (see Fig. 7, inset), we find that the mean values are more separated ($\langle\tau^L\rangle = (102.2 \pm 38.1)$ ms and $\langle\tau^S\rangle = (-0.73 \pm 7.14)$ ms), and with broader distributions ($\sigma^L = (375.1 \pm 69.6)$ ms and $\sigma^S = (16.5 \pm 7.5)$ ms) as a consequence of the different redshift distributions of the short and long GRBs: the average redshift for the long GRB sample is $\langle z^L\rangle = 1.84$ whereas for the short GRB sample is $\langle z^S\rangle = 0.85$ (Salvaterra et al., 2012; D'Avanzo et al., 2014). The KS test gives a probability of 2% that they are drawn from the same population.

We considered all the GRBs with measured lags in our samples (long and short) that also have an estimate of the bolometric isotropic luminosity $L_{\rm iso}$ to investigate the relation between the spectral lag and the GRB luminosity, namely 45 long GRBs and 6 short GRBs. For the values of $L_{\rm iso}$ and its definition we refer to Nava et al. (2012) and D'Avanzo et al. (2014).

If we restrict our analysis to all long GRBs with positive spectral lag (23; 51% of the sample), we find that the luminosity significantly anti-correlates with the spectral lag (Pearson correlation coefficient $r = -0.68$, null-hypothesis probability $P = 3.8 \times 10^{-4}$). The best linear fit to the $\log(L_{\rm iso}) - \log[\tau_{RF}]$ correlation that accounts for the statistical uncertainties on both axes yields: $\log[L_{\rm iso}/(10^{52}\ {\rm erg\,s^{-1}})] = (0.42 \pm 0.11) + (-1.79 \pm 0.03)\log[\tau_{RF}/100\,{\rm ms}]$ (see Fig. 8, inset). The scatter perpendicular to the correlation is modelled with a Gaussian with standard deviation $\sigma = 0.65$.

However, when we add to the lag-luminosity plane also the 20 long GRBs with lag consistent with zero within errors, no correlation between $L_{\rm iso}$ and the spectral lag is anymore apparent (see Fig. 8). There are also two long GRBs with negative lag (GRB 061021 and GRB 080721; cyan arrows in Fig. 8).

Short GRBs of our sample do not occupy a separate region of the lag-luminosity plane when compared to the total sample of long GRBs (see Fig. 8), because neither their distribution of the spectral lag is significantly different from the long GRB one, nor the luminosity distributions (KS probability $P = 38\%$). Therefore, the lag-luminosity correlation is questioned by these findings.

7. Discussion and conclusions

The classical division of short and long GRBs based on the hardness ratio (HR) versus duration (T_{90}) plot (e.g. Kouveliotou et al., 1993) signals that the two populations might have different spectral properties. Indeed, the HR is a proxy of the spectral shape: the comparison of the spectral parameters (obtained from the fit of the time integrated spectra) of short and long GRBs shows that short events are harder than long ones due to (a) a harder peak energy $E_{\rm peak}$ and (b) a harder low energy spectral index α (Ghirlanda et al., 2004, 2009). However, any possible spectral diversity should also consider the possible different distance scales of the two populations. If short and long GRBs have different progenitors then SGRBs should be typically localised at lower redshifts with respect to long ones due to the delay time between their formation (as binary systems) and their merger. If we consider a typical redshift $z \sim 0.6$ for SGRBs and $z \sim 2.1$ for long ones, the comparison of the rest frame spectral properties shows that short and long GRBs have similar peak energies and they only differ for a harder low energy spectral component in short GRBs. Similar considerations should be extended also to the short/long divide (i.e. $T_{90} = 2$ s). It has been argued (Bromberg et al., 2012) that the characteristic timescale for the jet to drill out the progenitor star in long GRBs (i.e. ∼10 s) could be associated to the break in the differential duration distribution observed in the population of GRBs detected by different satellites. This argument has been used to quantify the percentage of contamination of long GRBs (produced by collap-

Please cite this article in press as: G. Ghirlanda et al., Are short Gamma Ray Bursts similar to long ones?, J. High Energ. Phys. (2015), http://dx.doi.org/10.1016/j.jheap.2015.04.002

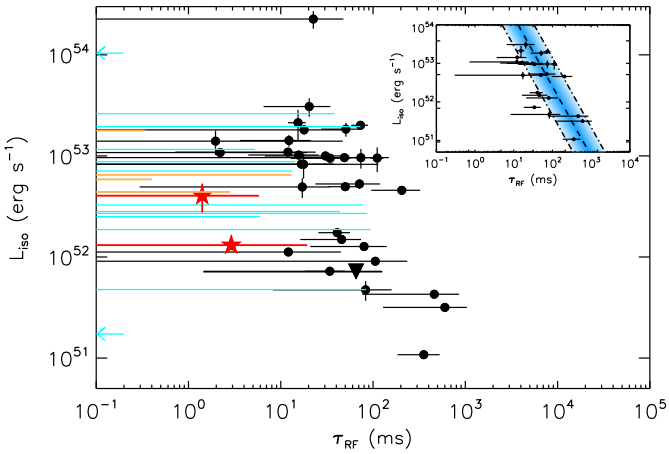

Fig. 8. Peak luminosity $L_{\rm iso}$ as a function of the rest-frame spectral lag. Black points: long GRBs with positive central value of the spectral lag (23 with positive lag and 9 with positive lag consistent with zero within errors). Cyan error bars: long GRBs with negative central value of the spectral lag (2 with negative lag, marked as left arrows, and 11 with negative lag consistent with zero within errors). Red stars: short GRBs with positive central value of the spectral lag (2 with positive lag consistent with zero within errors). Orange error bars: short GRBs with negative central value of the spectral lag (4 with negative lag consistent with zero within errors). The black triangle corresponds to GRB 100816A. Inset: lag-luminosity anti-correlation for the 23 long GRBs with positive lag. The black dashed line is the best fit to the data: $\log[L_{\rm iso}/(10^{52}\ {\rm erg\,s^{-1}})] = (0.42 \pm 0.11) + (-1.79 \pm 0.03)\log[\tau_{RF}/100\ {\rm ms}]$, and the blue area marks the 1σ region around the best fit. (For interpretation of the references to color in this figure legend, the reader is referred to the web version of this article.)

sar) in any sample of short GRBs selected solely for their observer frame duration. If again we consider the different distance scale of the two populations, however, the evidence of the break in the T_{90} distribution is highly reduced (Fig. 4).

The intrinsic properties of short and long GRBs show that they share similar luminosities and follow similar correlations in the $E_{\rm peak}$–$L_{\rm iso}$ plane. Short GRBs are less energetic than long events and they might define (although we still have few events) a parallel correlation to the $E_{\rm peak}$–$E_{\rm iso}$ defined by long events (Fig. 5). Despite still based on a limited number of events, these results have been obtained with complete well selected samples of long and short GRBs (Salvaterra et al., 2012; Nava et al., 2012; D'Avanzo et al., 2014). Therefore, for what concerns the time average (over the respective duration) spectral properties, short and long GRBs have similar luminosities and different energetics (i.e. proportional to the ratio of their average durations). However, GRBs show a considerable spectral evolution which seems to be similar in short and long events (Ghirlanda et al., 2011). When the spectra of short GRBs are compared to the time slices (of approximately the same size as the typical rest frame duration of short events) of long GRBs (Fig. 6) it appears that long GRBs start as short ones (Calderone et al., 2015).

Finally, it has been assumed for years that the spectral lag was a distinctive feature of short and long GRBs with the former having null lag (Norris et al., 2001; Norris and Bonnell, 2006). A detailed analysis (through the definition of complete samples of short and long GRBs with measured redshifts) of the spectral lags in the rest frame has shown (Fig. 7) that also long GRBs can have null lag (Bernardini et al., 2015). In the same line we could also show that the lag-luminosity correlation holding for long GRBs could have a large number of outliers since several long GRBs (∼50%) can have a null or negative lags.

All these considerations seem to point toward the possibility that short and long GRBs could be produced by different progenitors but the emission mechanism responsible for their prompt emission might be similar, with the exception of being able to produce a harder low energy spectral component in short events. If this is related to the spectral evolution, it might be that short GRBs are similar to the beginning of long events, where the longer duration of the central engine allows for the spectrum to evolve and become softer so that the overall time integrated spectrum also results softer. This would also suggest that the lags of long and short events should not be different as possibly demonstrated by our analysis.

Acknowledgments

G.G. and G.C. thank INAF/PRIN 2011 for financial support (grant number 1.05.01.09.15). The referee is acknowledged for useful comments. G. Ghisellini is acknowledged for stimulating discussions.

References

Abdo, A.A., Ackermann, M., Ajello, M., et al., 2009. Nature 462, 331–334.
Amati, L., et al., 2002. Astron. Astrophys. 390, 81.
Arimoto, M., Kawai, N., Asano, K., et al., 2010. Publ. Astron. Soc. Jpn. 62, 487.
Band, D., et al., 1993. Astrophys. J. 413, 281.
Band, D.L., 1997. Astrophys. J. 486, 928–937.
Barthelmy, S.D., Barbier, L.M., Cummings, J.R., et al., 2005. Space Sci. Rev. 120, 143–164.
Berger, E., 2014. Annu. Rev. Astron. Astrophys. 52, 43.
Bernardini, M.G., Margutti, R., Zaninoni, E., Chincarini, G., 2012. Mon. Not. R. Astron. Soc. 425, 1199.
Bernardini, M.G., Ghirlanda, G., Campana, S., et al., 2015. Mon. Not. R. Astron. Soc. 446, 1129–1138.
Bošnjak, Ž., Götz, D., Bouchet, L., Schanne, S., Cordier, B., 2014. Astron. Astrophys. 561, AA25.
Bromberg, O., Nakar, E., Piran, T., Sari, R., 2013. Astrophys. J. 764, 179.
Bromberg, O., Nakar, E., Piran, T., Sari, R., 2012. Astrophys. J. 749, 110.
Calderone, G., Ghirlanda, G., Ghisellini, G., Bernardini, M.G., Campana, S., Covino, S., D'Avanzo, V.D., Melandri, A., Salvaterra, R., Sbarufatti, B., Tagliaferri, G., 2015. There is a short gamma-ray burst prompt phase at the beginning of each long one. Mon. Not. R. Astron. Soc. 448, 403–416.
Cheng, L.X., Ma, Y.Q., Cheng, et al., 1995. Astron. Astrophys. 300, 746.
D'Avanzo, P., Salvaterra, R., Bernardini, M.G., 2014. arXiv:1405.5131.
de Ugarte Postigo, A., et al., 2011. Astron. Astrophys. 525, AA109.
Frontera, F., et al., 2009. Astrophys. J. Suppl. Ser. 180, 192.
Gehrels, N., Chincarini, G., Giommi, P., et al., 2004. Astrophys. J. 621, 558.
Gehrels, N., Norris, J.P., Barthelmy, S.D., et al., 2006. Nature 444, 1044–1046.
Ghirlanda, G., Celotti, A., Ghisellini, G., 2002. Astron. Astrophys. 393, 409.
Ghirlanda, G., Ghisellini, G., Celotti, A., 2004. Astron. Astrophys. 422, L55.
Ghirlanda, G., Nava, L., Ghisellini, G., Celotti, A., Firmani, C., 2009. Astron. Astrophys. 496, 585.
Ghirlanda, G., Ghisellini, G., Nava, L., 2011. Mon. Not. R. Astron. Soc. 418, L109.
Goldstein, A., Preece, R.D., Mallozzi, R.S., Briggs, M.S., Fishman, G.J., Kouveliotou, C., Paciesas, W.S., Burgess, J.M., 2013. Astrophys. J. Suppl. Ser. 208, 21.
Goldstein, A., et al., 2012. Astrophys. J. Suppl. Ser. 199, 19.
Golkhou, V.Z., Butler, N.R., 2014. Astrophys. J. 787, 90.
Gruber, D., et al., 2014. Astrophys. J. Suppl. Ser. 211, 12.
Guiriec, S., Briggs, M.S., Connaugthon, V., et al., 2010. Astrophys. J. 725, 225–241.
Guiriec, S., Daigne, F., Hascoët, R., et al., 2013. Astrophys. J. 770, 32.

Hakkila, J., Giblin, T.W., Norris, J.P., et al., 2008. Astrophys. J. Lett. 677, L81–L84.
Horváth, I., 1998. Astrophys. J. 508, 757.
Kaneko, Y., Preece, R.D., Briggs, M.S., Paciesas, W.S., Meegan, C.A., Band, D.L., 2006. Astrophys. J. Suppl. Ser. 166, 298.
Kouveliotou, C., Meegan, C.A., Fishman, G.J., Bhat, N.P., Briggs, M.S., Koshut, T.M., Paciesas, W.S., Pendleton, G.N., 1993. Astrophys. J. 413, L101.
Levan, A.J., et al., 2014. Astrophys. J. 781, 13.
MacLachlan, G.A., et al., 2013. Mon. Not. R. Astron. Soc. 432, 857.
MacLachlan, G.A., Shenoy, A., Sonbas, E., Dhuga, K.S., Eskandarian, A., Maximon, L.C., Parke, W.C., 2012. Mon. Not. R. Astron. Soc. 425, L32.
Margutti, R., Guidorzi, C., Chincarini, G., et al., 2010. Mon. Not. R. Astron. Soc. 406, 2149–2167.
Margutti, R., et al., 2013. Mon. Not. R. Astron. Soc. 428, 729.
Nakar, E., Piran, T., 2002. Mon. Not. R. Astron. Soc. 330, 920.
Nava, L., Ghirlanda, G., Ghisellini, G., Celotti, A., 2011a. Mon. Not. R. Astron. Soc. 415, 3153.
Nava, L., Ghirlanda, G., Ghisellini, G., Celotti, A., 2011b. Astron. Astrophys. 530, AA21.
Nava, L., Salvaterra, R., Ghirlanda, G., et al., 2012. Mon. Not. R. Astron. Soc. 421, 1256–1264.
Norris, J.P., 2002. Implications of the lag-luminosity relationship for unified gamma-ray burst paradigms. Astrophys. J. 579, 386–403.
Norris, J.P., Bonnell, J.T., 2006. Astrophys. J. 643, 266–275.
Norris, J.P., Marani, G.F., Bonnell, J.T., 2000. Astrophys. J. 534, 248–257.
Norris, J.P., Scargle, J.D., Bonnell, J.T., 2001. In: Costa, E., Frontera, F., Hjorth, J. (Eds.), Gamma-Ray Bursts in the Afterglow Era, p. 40.
Norris, J., Ukwatta, T.N., Barthelmy, S.D., Gehrels, N., Stamatikos, M., Sakamoto, T., 2010. GCN 11113, 1.
Preece, R.D., Briggs, M.S., Mallozzi, R.S., Pendleton, G.N., Paciesas, W.S., Band, D.L., 2000. Astrophys. J. Suppl. Ser. 126, 19.
Pélangeon, A., et al., 2008. Astron. Astrophys. 491, 157.
Qin, Y., et al., 2013. Astrophys. J. 763, 15.
Qin, Y.-P., Xie, G.-Z., Liang, E.-W., Zheng, X.-T., 2001. Astron. Astrophys. 369, 537.
Řípa, J., Mészáros, A., Wigger, C., Huja, D., Hudec, R., Hajdas, W., 2009. Astron. Astrophys. 498, 399.
Salvaterra, R., Campana, S., Vergani, S.D., et al., 2012. Astrophys. J. 749, 68.
Sakamoto, T., et al., 2005. Astrophys. J. 629, 311.
Sakamoto, T., et al., 2011. Astrophys. J. Suppl. Ser. 195, 2.
Savchenko, V., Neronov, A., Courvoisier, T.J.-L., 2012. Astron. Astrophys. 541, AA122.
Schaefer, B.E., 2007. Astrophys. J. 660, 16–46.
Tavani, M., 1998. Astrophys. J. 497, L21.
Tsutsui, R., Yonetoku, D., Nakamura, T., Takahashi, K., Morihara, Y., 2013. Mon. Not. R. Astron. Soc. 431, 1398.
Ukwatta, T.N., Dhuga, K.S., Stamatikos, M., et al., 2012. Mon. Not. R. Astron. Soc. 419, 614–623.
Ukwatta, T.N., Stamatikos, M., Dhuga, K.S., et al., 2010. Astrophys. J. 711, 1073–1086.
von Kienlin, A., et al., 2014. Astrophys. J. Suppl. Ser. 211, 13.
Zhang, F.-W., Shao, L., Yan, J.-Z., Wei, D.-M., 2012. Astrophys. J. 750, 88.
Yonetoku, D., Murakami, T., Nakamura, T., Yamazaki, R., Inoue, A.K., Ioka, K., 2004. Astrophys. J. 609, 935.

Please cite this article in press as: G. Ghirlanda et al., Are short Gamma Ray Bursts similar to long ones?, J. High Energ. Phys. (2015), http://dx.doi.org/10.1016/j.jheap.2015.04.002